

The $B \rightarrow \pi l \nu$ form factor from unquenched lattice QCD with domain-wall light quarks and relativistic b -quarks

Taichi Kawanai*

Physics Department, Brookhaven National Laboratory, Upton, NY 11973, USA

RIKEN-BNL Research Center, Brookhaven National Laboratory, Upton, NY 11973, USA

Department of Physics, The University of Tokyo, Hongo 7-3-1, Tokyo 113-0033, Japan

E-mail: kawanai@nt.phys.s.u-tokyo.ac.jp

Ruth S. Van de Water

Physics Department, Brookhaven National Laboratory, Upton, NY 11973, USA

Theoretical Physics Department, Fermi National Accelerator Laboratory, Batavia, IL 60510, USA

E-mail: ruthv@fnal.gov

Oliver Witzel

Center for Computational Science, Boston University, 3 Cummington Mall, Boston, MA 02215, USA

E-mail: owitzel@bu.edu

We report on a lattice-QCD calculation of the $B \rightarrow \pi l \nu$ form factor with domain-wall light quarks and relativistic b -quarks using the $2 + 1$ flavor domain-wall fermion and Iwasaki gauge-field ensembles generated by the RBC and UKQCD Collaborations. We present initial results obtained from the coarser ($a \approx 0.11$ fm) 24^3 lattices and some of the finer ($a \approx 0.086$ fm) 32^3 lattices.

*The 30 International Symposium on Lattice Field Theory - Lattice 2012,
June 24-29, 2012
Cairns, Australia*

*Speaker.

1. Introduction

The theoretical calculation of the hadronic $B \rightarrow \pi l \nu$ form factor $f_+(q^2)$ is a key ingredient in the determination of the Cabibbo-Kobayashi-Maskawa (CKM) matrix element $|V_{ub}|$ from $B \rightarrow \pi l \nu$ exclusive semi-leptonic decay. The value of $|V_{ub}|$ characterizes the strength of the quark-flavor changing $b \rightarrow u$ transition, and can be obtained by combining the hadronic $B \rightarrow \pi l \nu$ form factor $f_+(q^2)$ with experimental measurements of the differential decay rate via

$$\frac{d\Gamma(B \rightarrow \pi l \nu)}{dq^2} = \frac{G_F^2 |V_{ub}|^2}{192\pi^2 m_B^3} [(m_B^2 + m_\pi^2 - q^2)^2 - 4m_B^2 m_\pi^2]^{3/2} |f_+(q^2)|^2, \quad (1.1)$$

where the momentum transfer $q^\mu \equiv p_B^\mu - p_\pi^\mu$ and we neglect the mass of the outgoing lepton. The form factor $f_+(q^2)$ encodes nonperturbative QCD dynamics, and can only be computed precisely from first principles using lattice QCD. Indeed there have been two $2+1$ flavor lattice calculations of $f_+(q^2)$ done by the HPQCD [1] and FNAL/MILC Collaborations [2]. Both groups use the MILC gauge configurations.

The precise calculation of $|V_{ub}|$ constrains the apex of the CKM unitarity triangle. There is a persistent puzzle, however, between independent determinations of $|V_{ub}|$. First, the exclusive determination from $B \rightarrow \pi l \nu$ and the inclusive determination from $B \rightarrow X_u l \nu$ (where X_u is any charmless hadronic final state) differ at the level of more than 3σ [3]. Second, most experimental measurements of BR ($B \rightarrow \tau \nu$) combined with lattice-QCD input for f_B give a higher value of $|V_{ub}|$ than both $|V_{ub}|_{\text{excl}}$ and $|V_{ub}|_{\text{incl}}$ [4, 5], although the recent Belle measurement of BR ($B \rightarrow \tau \nu$) is lower and more in line with the Standard-Model prediction, albeit still with large errors [6]. Given this situation, an independent lattice calculation using a different gauge action is desired to address this puzzle.

2. Methodology

The $B \rightarrow \pi l \nu$ hadronic weak matrix element is parameterized by the form factors $f_+(q^2)$ and $f_0(q^2)$ as

$$\langle \pi | \mathcal{V}^\mu | B \rangle = f_+(q^2) \left(p_B^\mu + p_\pi^\mu - \frac{m_B^2 - m_\pi^2}{q^2} q^\mu \right) f_0(q^2) \frac{m_B^2 - m_\pi^2}{q^2} q^\mu, \quad (2.1)$$

where the $b \rightarrow u$ vector current $\mathcal{V}^\mu \equiv i\bar{u}\gamma^\mu b$. We calculate numerically the form factors f_\parallel and f_\perp , which are more convenient for the lattice calculation:

$$\langle \pi | \mathcal{V}^\mu | B \rangle = \sqrt{2m_B} [v^\mu f_\parallel(E_\pi) + p_\perp^\mu f_\perp(E_\pi)], \quad (2.2)$$

where $v^\mu = p_B^\mu/m_B$ and $p_\perp^\mu = p_\pi^\mu - (p_\pi \cdot v)v^\mu$. In the B -meson rest frame, these form factors are proportional to the hadronic matrix elements of the temporal and spatial vector current:

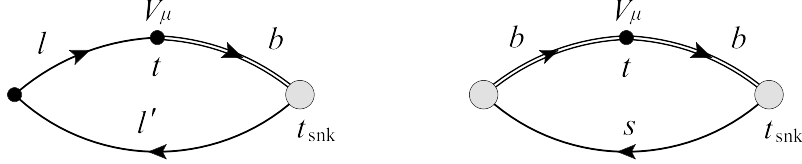
$$f_\parallel = \frac{\langle \pi | \mathcal{V}^0 | B \rangle}{\sqrt{2m_B}}, \quad f_\perp = \frac{\langle \pi | \mathcal{V}^i | B \rangle}{\sqrt{2m_B}} \frac{1}{p_\pi^i}. \quad (2.3)$$

The desired form factor f_+ can be obtained by following relation:

$$f_+(q^2) = \frac{1}{\sqrt{2m_B}} [f_\parallel(E_\pi) + (m_B - E_\pi) f_\perp(E_\pi)]. \quad (2.4)$$

Table 1: Lattice simulation parameters. The results reported here use the ensembles specified in boldface

a [fm]	$L^3 \times T$	am_l	am_s	M_π [MeV]	# configs.	# time sources
$\approx \mathbf{0.11}$	$\mathbf{24^3 \times 64}$	$\mathbf{0.005}$	$\mathbf{0.040}$	$\mathbf{329}$	$\mathbf{1636}$	$\mathbf{1}$
$\approx \mathbf{0.11}$	$\mathbf{24^3 \times 64}$	$\mathbf{0.010}$	$\mathbf{0.040}$	$\mathbf{422}$	$\mathbf{1419}$	$\mathbf{1}$
$\approx \mathbf{0.086}$	$\mathbf{32^3 \times 64}$	$\mathbf{0.004}$	$\mathbf{0.030}$	$\mathbf{289}$	$\mathbf{628}$	$\mathbf{2}$
≈ 0.086	$32^3 \times 64$	0.006	0.030	345	889	2
≈ 0.086	$32^3 \times 64$	0.008	0.030	394	544	2

**Figure 1:** Three-point correlation functions for computing the $B \rightarrow \pi l \nu$ form factor (left) and renormalization factor Z_V^{bb} (right). The single and double lines correspond to light- and b -quark propagators, respectively. The spectator light quark is labeled l' and the daughter light quark is labeled l . Shaded circles denote the gauge invariant Gaussian smeared source/sink for the b -quarks.

We match the lattice amplitude to the continuum matrix element using the mostly nonperturbative method of Ref. [7]:

$$\langle \pi | \mathcal{V}^\mu | B \rangle = Z_V^{bl} \langle \pi | V^\mu | B \rangle, \quad Z_V^{bl} = \rho_{V_\mu}^{bl} \sqrt{Z_V^{bb} Z_V^{ll}}. \quad (2.5)$$

The flavor-conserving renormalization factors Z_V^{bb} and Z_V^{ll} are computed nonperturbatively on the lattice and the factor ρ is computed at one loop in mean-field improved lattice perturbation theory [8]. Most of the heavy-light current renormalization factor comes from Z_V^{bb} and Z_V^{bl} , such that ρ is expected to be close to unity [9].

We improve the $b \rightarrow u$ vector current through $\mathcal{O}(\alpha_s a)$. At this order we need only compute one additional matrix element with a single-derivative operator. We calculate the improvement coefficient at 1-loop in mean-field improved lattice perturbation theory. We have not yet included the $\mathcal{O}(a)$ -improvement term in the results shown in these proceedings.

3. Computational setup

Our computation of the $B \rightarrow \pi l \nu$ form factor is performed on $2+1$ flavor domain-wall fermion and Iwasaki gauge-field ensembles generated by the RBC and UKQCD Collaborations with several values of the light dynamical quark mass at two lattice spacings, the coarser $a \approx 0.11$ fm ($a^{-1} \approx 1.73$ GeV) and the finer $a \approx 0.086$ fm ($a^{-1} \approx 2.28$ GeV) [10, 11]. The set of gauge-field configurations used for this project is summarized in Table 1. The results reported here use the ensembles specified in boldface. On the finer ensembles we compute two quark propagators on each configuration with their temporal source locations separated by $T/2$ to increase the statistics. Periodic boundary conditions are imposed in the time direction. In this proceedings, we present first results obtained from the coarser ensembles and a subset of the finer ensembles.

For the light quarks, domain-wall valence quark propagators are generated on each configurations with several partially quenched masses in order to enable good control over the chiral extrapolation. For the bottom quark, we use the relativistic heavy quark (RHQ) action [12] to remove the large discretization error introduced by the large bottom quark mass [13]. The RHQ action is given by

$$S_{\text{RHQ}} = \sum_{n,m} \bar{q}_n \left\{ m_0 + \gamma_0 D_0 - \frac{aD_0^2}{2} + \xi \left[\vec{\gamma} \cdot \vec{D} - \frac{a(\vec{D})^2}{2} \right] - a \sum_{\mu,\nu} \frac{ic_P}{4} \sigma_{\mu\nu} F_{\mu\nu} \right\} q_m \quad (3.1)$$

where tuning the bare-quark mass $m_0 a$, the clover coefficient c_P , and the anisotropy parameter ξ for the b quark is needed [12, 14]. Here we employ values determined nonperturbatively in Ref. [15].

Figure 1 shows the the three-point correlation functions needed in this project. The left diagram of Fig. 1 depicts the computation of the $B \rightarrow \pi l \nu$ form factor. The source of the pion (with both zero and nonzero momenta) is located at the origin. The B -meson is at rest at t_{snk} . We compute this three-point function with a unitary spectator mass and multiple partially quenched daughter-quark masses that enable interpolation to the physical strange-quark mass and extrapolation to the physical average up-down quark mass. The right diagram of Fig. 1 is used to obtain the renormalization factor Z_V^{bb} . We fix the the spectator mass to be $m_q = m_s$ in order to reduce the statistical errors because Z_V^{bb} is independent of the light spectator-quark mass. For Z_V^{ll} , we use the value obtained by the RBC/UKQCD Collaborations in Ref. [11]. To reduce excited-state contamination, we employ a gauge-invariant Gaussian smeared (sequential) source for the B -meson in all lattice correlators. In order to reduce the statistical error of the three point function, we calculate the three point function with the B -meson at t_{snk} and $(T - t_{\text{snk}})$ and average the results.

4. Two-point and three-point fits

The pion energy and B -meson mass are obtained from the following two point functions:

$$C_2^\pi(t, \vec{p}) = \sum_{\vec{x}} e^{i\vec{p} \cdot \vec{x}} \langle \mathcal{O}_\pi(t, \vec{x}) \mathcal{O}_\pi^\dagger(0, \vec{0}) \rangle, \quad (4.1)$$

$$C_2^B(t) = \sum_{\vec{x}} \langle \mathcal{O}_B(t, \vec{x}) \mathcal{O}_B^\dagger(0, \vec{0}) \rangle, \quad (4.2)$$

where \mathcal{O}_π and \mathcal{O}_B are interpolating operators for the pion and B -meson. We compute the effective energies as

$$E_{\text{eff}}(\vec{p}) = \cosh^{-1} \left[\frac{C_2(t, \vec{p}) + C_2(t+2, \vec{p})}{C_2(t+1, \vec{p})} \right]. \quad (4.3)$$

The left plot of Fig. 2 shows the effective pion energies for momenta through $(\vec{p}L/2\pi)^2 = 3$ on the the coarser $am_l = 0.005$ ensemble. Similarly, the right plot of Fig. 2 shows the effective B -meson mass calculated with a Gaussian smeared source and point sink.

In the lattice-QCD simulations, the form factors $f_{\parallel}^{\text{lat}}$ and f_{\perp}^{lat} can be obtained from the following ratios of correlation functions:

$$R_{3,\mu}^{B \rightarrow \pi}(t, t_{\text{snk}}) = \frac{C_{3,\mu}^{B \rightarrow \pi}(t, t_{\text{snk}})}{\sqrt{C_2^\pi(t) C_2^B(t_{\text{snk}} - t)}} \sqrt{\frac{2E_\pi}{e^{-E_\pi t} e^{-m_B t}}} \quad (4.4)$$

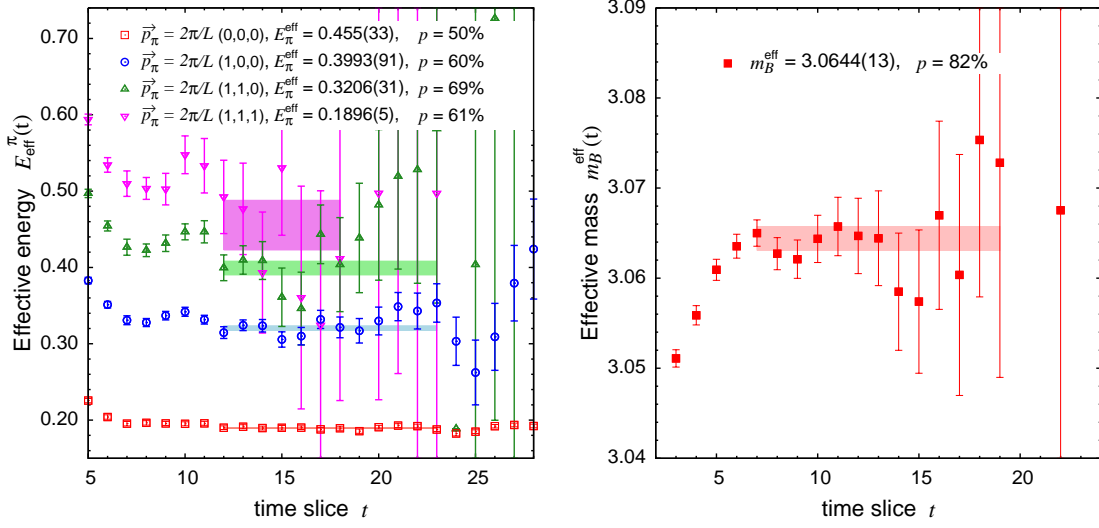


Figure 2: Effective energy/mass plots for the pion (left) and B -meson (right) on the coarser $am_l = 0.005$ ensemble. Shaded bands show the fit results with jackknife statistical errors and fit ranges. For the pion, data points for four spatial momenta $(\vec{p}_L/2\pi)^2 = 0, 1, 2, 3$ are indicated by different colors/symbols.

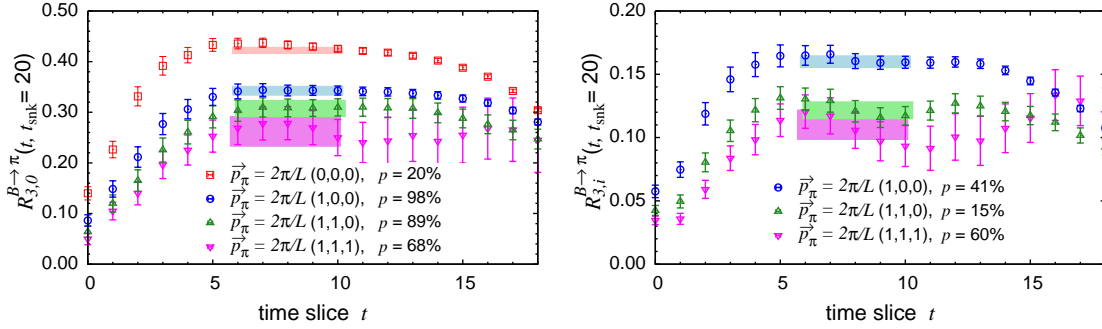


Figure 3: The ratio $R_{3,0}^{B \rightarrow \pi}$ (left) and $R_{3,i}^{B \rightarrow \pi}$ (right) with $t_{\text{snk}} = 20$ on the coarser $am_l = 0.005$ ensemble. Fit ranges and fit results with jackknife statistical errors are shown as horizontal bands.

$$f_{\parallel}^{\text{lat}} = \lim_{0 \ll t \ll t_{\text{snk}}} R_0^{B \rightarrow \pi}(t, t_{\text{snk}}), \quad (4.5)$$

$$f_{\perp}^{\text{lat}} = \lim_{0 \ll t \ll t_{\text{snk}}} \frac{1}{p_{\pi}^i} R_i^{B \rightarrow \pi}(t, t_{\text{snk}}), \quad (4.6)$$

where

$$C_{3,\mu}^{B \rightarrow \pi}(t, t_{\text{snk}}, \vec{p}) = \sum_{\vec{x}, \vec{y}} e^{i\vec{p}_{\pi} \cdot \vec{y}} \langle \mathcal{O}_B(t_{\text{snk}}, \vec{x}) V_{\mu}(t, \vec{y}) \mathcal{O}_{\pi}^{\dagger}(0, \vec{0}) \rangle. \quad (4.7)$$

V_{μ} is the vector current matrix element on the lattice.

Fig. 3 shows the results for $R_{3,0}^{B \rightarrow \pi}$ and $R_{3,i}^{B \rightarrow \pi}$ calculated with a source-sink separation $t_{\text{snk}} = 20$ on the coarser $am_l = 0.005$ ensemble. For $R_{3,i}^{B \rightarrow \pi}$, we average over equivalent spatial momenta. Plots of these ratios for the other ensembles and partially quenched masses look similar. We determine $f_{\parallel}^{\text{lat}}$ and f_{\perp}^{lat} by fitting to a plateau in the region $0 \ll t \ll t_{\text{snk}}$ where we expect the excited-state contributions to be negligible and obtain a good correlated $\chi^2/\text{d.o.f.}$ and p -value.

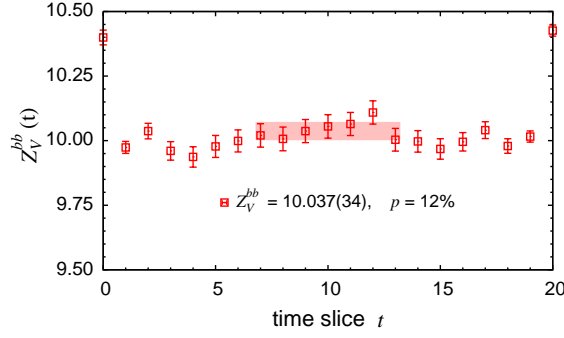


Figure 4: Determination of the renormalization factor Z_V^{bb} with $t_{\text{snk}} = 20$ on the coarser $am_l = 0.005$ ensemble. The shaded band shows the fit result with jackknife statistical error.

5. Renormalization factor Z_V^{bb}

Values of Z_V^{bb} can be computed nonperturbatively using the charge-normalization condition $Z_V^{bb} \langle B_s | V^{bb,0} | B_s \rangle = 1$ where $V^{bb,0}$ is the $b \rightarrow b$ lattice vector current. We obtain Z_V^{bb} by fitting the following ratio of correlators to a plateau in a region $0 \ll t \ll t_{\text{snk}}$:

$$Z_V^{bb}(t, t_{\text{snk}}) = C_2^{B_s}(t_{\text{snk}}) / C_{3,0}^{B_s \rightarrow B_s}(t, t_{\text{snk}}). \quad (5.1)$$

The determination of Z_V^{bb} on the coarser $am_l = 0.005$ ensemble is shown in Fig. 5. At tree level in mean-field improved lattice perturbation theory, Z_V^{bb} is given by [12, 13]

$$Z_V^{bb} = u_0 \exp(M_1), \quad M_1 = \log[1 + \tilde{m}_0], \quad \tilde{m}_0 = \frac{m_0}{u_0} - (1 + 3\zeta)(1 - \frac{1}{u_0}). \quad (5.2)$$

Using $m_0 = 8.45$, $\zeta = 3.1$ and $u_0 = 0.8757$ for the coarser $am_l = 0.005$ ensemble [11, 15], we obtain a tree level estimate $Z_V^{bb} = 10.606$, which is in good agreement with the nonperturbative determination.

6. Form-factor results and outlook

After multiplying the results for $R_{3,0}^{B \rightarrow \pi}$ and $R_{3,i}^{B \rightarrow \pi}$ with the renormalization factor Z_V^{bl} , we obtain the form factors f_{\parallel} and f_{\perp} shown in Fig. 5. (For now the ρ -factor is set to unity.) After adding the ρ -factors and $\mathcal{O}(a)$ -improvement, we will extrapolate to the physical quark masses and continuum and interpolate in E_{π}^2 using chiral perturbation theory. Calculations on the remaining finer ensembles are underway.

We will then extrapolate our synthetic form-factor data over the full kinematic range (down to $q^2 = 0$) using the model-independent z -parameterization [16–19]. Our result will provide an important independent check on existing calculations using staggered light quarks.

7. Acknowledgments

We thank our collaborators in the RBC and UKQCD Collaborations for helpful discussions. Computations for this work were mainly performed on resources provided by the USQCD Col-

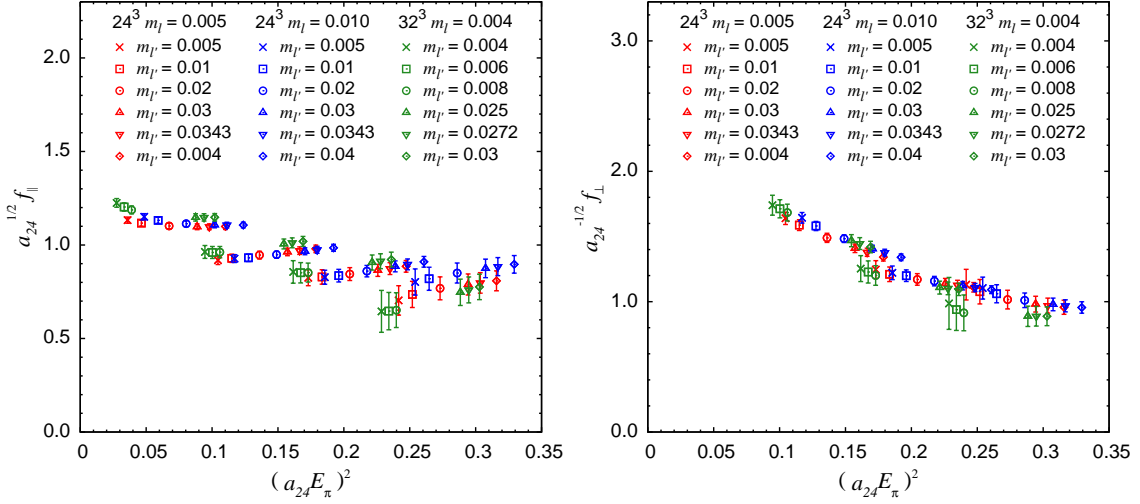


Figure 5: Form factors f_{\parallel} and f_{\perp} in coarse lattice units a_{24} . The red, blue and green symbols indicate data on the coarser $am_l = 0.005$, $am_l = 0.01$ and finer $am_l = 0.004$ ensembles, respectively. Different symbols indicate different partially quenched masses.

laboration, funded by the Office of Science of the U.S. Department of Energy, as well as computers at BNL and Columbia University. T.K. is partially supported by JSPS Grants-in-Aid (No. 22-7653). O.W. acknowledges support at Boston University by the U.S. DOE grant DE-FC02-06ER41440. BNL is operated by Brookhaven Science Associates, LLC under Contract No. DE-AC02-98CH10886 with the U.S. Department of Energy. Fermilab is operated by Fermi Research Alliance, LLC, under Contract No. DE-AC02-07CH11359 with the U.S. Department of Energy.

References

- [1] E. Dalgic *et al.*, *Phys.Rev.* **D73**, 074502 (2006)
- [2] J. A. Bailey *et al.*, *Phys.Rev.* **D79**, 054507 (2009)
- [3] M. Antonelli *et al.*, *Phys.Rept.* **494**, 197 (2010)
- [4] E. Lunghi and A. Soni, *Phys.Lett.* **B697**, 323 (2011)
- [5] J. Laiho, E. Lunghi, and R. Van de Water, *PoS LATTICE2011*, 018 (2011)
- [6] I. Adachi *et al.* (Belle Collaboration)(2012), [arXiv:1208.4678 \[hep-ex\]](#)
- [7] A. X. El-Khadra *et al.*, *Phys.Rev.* **D64**, 014502 (2001)
- [8] G. P. Lepage and P. B. Mackenzie, *Phys.Rev.* **D48**, 2250 (1993)
- [9] J. Harada *et al.*, *Phys.Rev.* **D65**, 094513 (2002)
- [10] C. Allton *et al.* (RBC-UKQCD Collaboration), *Phys.Rev.* **D78**, 114509 (2008)
- [11] Y. Aoki *et al.* (RBC Collaboration, UKQCD Collaboration), *Phys.Rev.* **D83**, 074508 (2011)
- [12] N. H. Christ, M. Li, and H.-W. Lin, *Phys.Rev.* **D76**, 074505 (2007)
- [13] A. X. El-Khadra, A. S. Kronfeld, and P. B. Mackenzie, *Phys.Rev.* **D55**, 3933 (1997)
- [14] H.-W. Lin and N. Christ, *Phys.Rev.* **D76**, 074506 (2007)
- [15] Y. Aoki *et al.* (RBC Collaboration, UKQCD Collaboration)(2012), [arXiv:1206.2554 \[hep-lat\]](#)
- [16] C. Bourrely, B. Machet, and E. de Rafael, *Nucl.Phys.* **B189**, 157 (1981)
- [17] C. G. Boyd, B. Grinstein, and R. F. Lebed, *Phys.Rev.Lett.* **74**, 4603 (1995)
- [18] M. C. Arnesen, B. Grinstein, I. Z. Rothstein, and I. W. Stewart, *Phys.Rev.Lett.* **95**, 071802 (2005)
- [19] C. Bourrely, I. Caprini, and L. Lellouch, *Phys.Rev.* **D79**, 013008 (2009)